

**2021 NDIA GROUND VEHICLE SYSTEMS ENGINEERING AND TECHNOLOGY
SYMPOSIUM
SURVIVABILITY TECHNICAL SESSION
AUGUST 10-12, 2021 - NOVI, MICHIGAN**

Developing Performance and Operating Requirements for Energy Attenuation (EA) Roof Liners for all U.S. Army Military Vehicles

Julie Klima

U.S. Army Ground Vehicle Systems Center, Warren, MI

ABSTRACT

The primary focus of this effort is to evaluate the roof liner technology's ability to reduce the head injury criteria (HIC) and head acceleration to mitigate vertical impact related injuries to mounted crew injuries which may occur during top and bottom threat events. In an effort to reduce the likelihood of head injury during top and bottom threat attacks, an adequate roof liner is needed to reduce the force exerted on the soldier. The roof liners were able to pass all system level tests. The successful system level testing confirmed the blast mat technology's TRL-6 recommendation.

Citation: J. Klima, "Developing Performance and Operating Requirements for Energy Attenuating (EA) Roof Liner for all U.S. Army Military Vehicles", In *Proceedings of the Ground Vehicle Systems Engineering and Technology Symposium (GVSETS)*, NDIA, Novi, MI, Aug. 10-12, 2021.

1. INTRODUCTION

The U.S. Army Ground Vehicle Systems Center (GVSC) Ground Vehicle Survivability and Protection (GVSP) Occupant Protection Team (OPT) has worked to develop a Military Performance Specification, MIL-PRF-32518A. This specification established performance and operating requirements for energy attenuating (EA) roof liners used for U.S. Army military vehicles and reporting procedures for requirement verification. Mounted soldiers experience threats from multiple directions; these threats produce rapid and violent displacement of the vehicle. Vehicle interior structures are typically made of rigid, thick armor and angular, unfriendly surfaces. Vehicle interiors are not conducive to warfighter safety

during threat events. EA roof liners can reduce the risk of injury [2] to occupants during vertical accelerative loading events.

This paper details the various testing and research that went into finding the appropriate roof liner technology criteria that meets within the guidelines of a military vehicle environment. Mounted soldiers experience top and bottom attack events when an evolving threat is detonated above and below the military vehicle. The resulting wave produces a rapid and violent displacement of the vehicle. U.S. Army vehicle interior structures are typically made of rigid, thick, armor and angular surfaces. The primary focus of this effort is to evaluate the roof liner technology's ability to reduce the head resultant and head injury criteria (HIC) to mitigate vertical impact related injuries to mounted crew. The study is limited to mounted crews, which are assumed to be seated and properly restrained inside the vehicle.

2. BACKGROUND

The research shown throughout this paper was conducted from 2013 to present, 2021. Upon completion on the commercial off the shelf (COTS) EA roof liner head impact testing and the flame, smoke, and toxicity (FST) testing, it was evident that there was currently not a COTS material that could meet both sets of requirements.

As a result the Army's Small Business Innovation Research (SBIR) was used create a roof liner technology that met the required head injury criteria in addition to military environment FST requirements. The Phase 1 SBIR program was kicked off from June to December 2014, the Phase I Option was from August to November 2015, and the Phase 2 SBIR was January 2016 to December 2017. The roof liner technology resulting from the SBIR program has demonstrated meeting all requirements proposed. The roof liner technology resulting from the SBIR program was used for attachment method testing in addition to vibration studies explored in this paper.

The velocity input was found in collaboration with the Warrior Injury Assessment Manikin (WIAMan) project [4]. Ground Vehicle Systems Center (GVSC) used the knowledge gained from this project to provide a roof liner recommendation for the performance specification.

3. METHODOLOGY

3.1. Injury Criteria

Head Injury Criteria (HIC) was used as the head injury tolerance leveraging the automotive industry Society of Automotive Engineers (SAE) TP201U-01, FMVSS 201U [1] for Occupant Protection in Interior Impact Upper Interior Head Impact Protection. The HIC(d) shall not exceed 1000 when calculated in accordance with the following formula:

$$HIC = \left[\frac{1}{t_2 - t_1} \int_{t_1}^{t_2} a(t) dt \right]^{2.5} (t_2 - t_1) [1]$$

Where t_1 and t_2 are points in time of no more than 36 ms of separation and AR is equal to the sum of resultant acceleration magnitude in g units at the free motion headform center of gravity.

Head injury criteria of 1000 is roughly a sixteen percent likelihood of skull fracture according to Prasad and Mertz study conducted in 1985 [12]. A HIC of 1000 equates to an abbreviated injury scale (AIS) greater than or equal to three.

3.2. Head Impact COTS Material

The free motion headform (FMH) targeted impact speed is 24 kph \pm 1.0 kph. The FMH velocity was derived from cadaveric underbody blast (UBB) testing conducted by the Warrior Injury Assessment Manikin (WIAMan) program at Aberdeen Proving Ground (APG) Aberdeen, Maryland.

Measurement system analysis was conducted with and without the use of an Army combat helmet (ACH) mounted onto the Free Motion Headform Figure 1. The results of this analysis was that the use of an ACH with the FMVSS 201U test equipment had too much variation for repeatability. Testing was conducted without an ACH where applicable. During baseline testing, certain impact target locations would damage the skin on the FMH in these instances an ACH was used during testing. The expectation is that testing conducted without an ACH would have higher HIC(d) values and it is assumed that mounted warfighters are always wearing their ACH when in theater.



Figure 1: Head impact fixture

The core materials target thickness range from 25.4 mm (1.0 inch) to 38.1 mm (1.5 inches) was based on occupant space claim in the military vehicles. The core materials' thickness tested ranged from 12.7 mm (0.50 inches) to 41 mm (1.6 inches). The range varied due to availability to procure COTS material. Both fabric and rigid exposed surface sheet materials were assembled to the energy attenuating materials for head impact testing. Table 1 illustrates the material test matrix used in testing the COTS materials.

GVSC tested different commercial off the shelf (COTS) energy attenuating (EA) core materials at the SANG Subsystem Impact Simulator SSII laboratory using a rigid flat fixture, Figure 2. The core material requires an additional layer of protection for durability. The additional durable layer of material is referred to by GVSC as an exposed surface sheet. Each core material was tested with a different durable exposed surface sheet to understand the effects the exposed surface sheet had on the energy attenuation characterizes of the core materials.



Figure 2: Rigid Flat Fixture

Table 1: Analysis of Alternates (AoA) Material Test Matrix

Core Material ID	Facesheet Material ID	Facesheet Material	Material	Thickness
A	1	Fabric	Plastic	1.4 inch (35.5 mm)
A	2	Fabric		
A	3	Fabric		
A	4	Fabric		
B	1	Fabric	Plastic	0.8 inch (20.3 mm)
B	2	Fabric		
B	3	Fabric		
B	4	Fabric		
C	1	Fabric	Plastic	0.5 inch (12.7 mm)
C	2	Fabric		
C	3	Fabric		
C	4	Fabric		
C	5	Rigid		
D	1	Fabric	Plastic	1.5 inch (38.1 mm)
D	2	Fabric		
D	3	Fabric		
D	4	Fabric		
D	5	Rigid		
D	6	Fabric		
E	1	Fabric	Plastic	1.5 inch (38.1 mm)
E	2	Fabric		
E	3	Fabric		
E	4	Fabric		
E	5	Rigid		
F	1	Fabric	Plastic	0.5 inch (12.7 mm)
F	2	Fabric		
F	3	Fabric		
F	4	Fabric		
F	5	Rigid		
G	1	Fabric	Foam	1.0 inch (25.4 mm)
G	2	Fabric		
G	3	Fabric		
G	4	Fabric		
G	7	Fabric		
H	1	Fabric	Foam	0.5 inch (12.7 mm)
H	2	Fabric		
H	3	Fabric		
H	4	Fabric		
H	7	Fabric		
I	1	Fabric	Non-resilient	1.6 inch (40.6 mm)
I	2	Fabric		
I	3	Fabric		
I	4	Fabric		
I	5	Rigid		
J	1	Fabric	Non-resilient	0.78 inch (19.8 mm)
J	2	Fabric		
J	3	Fabric		
J	4	Fabric		
J	5	Rigid		
J	8	Rigid		

The core and exposed face sheet materials were conditioned before testing. The material samples were soaked in an ambient air environment of 19°C to 26°C (66.2°F to 78.8°F) and a relative humidity between 10 percent and 70 percent. [1]

3.3. Flame, Smoke, and Toxicity (FST)

GVSC developed FST requirements based upon communication with subject matter experts from the Naval Sea Systems Command (NAVSEA) and GVSC’s Automatic Fire Extinguishing System (AFES) Group. The standards and criteria represent more severe fire ignition sources such as are likely to occur in U.S. Army vehicles. Table 1 illustrates the flame, smoke, and toxicity criterion used in testing the commercial off the shelf (COTS) materials.

Table 2: Flame, Smoke, and Toxicity Criteria

Requirement	Threshold	Test Method
Avg. Peak Heat Release Rate 50 kW/m ²	< 85 kW/m ²	ASTM E 1354
Peak Heat Release Rate after ignition 50 kW/m ² @ 20 s, 180 s, & 300 s	< 60 kW/m ²	
Flame Spread Index	< 30	ASTM E 162
Smoke Density Flaming @240 S	D _m < 200	ASTM E 662
Smoke Density Non-Flaming @ 240 s		

GVSC contracted a third party laboratory to perform the flame, smoke, and toxicity testing of COTS materials. The core material requires an additional layer of protection for durability. The additional durable layer of material is referred to by GVSC as a facesheet material. The core materials’ thickness tested ranged from 12.7 mm (0.50 inch) to 38.1 mm (1.5 inch). The material thickness was based on occupant space claim in the military vehicles. Both fabric and rigid exposed surface sheet materials were assembled to the energy attenuating materials for flame, smoke, and toxicity testing. Table 2 illustrates the material test matrix used in testing the COTS materials.

Table 3: Material Test Matrix

		Material ID	Material	Thickness
Core Material ID		A	Plastic	0.8"
		B	Foam	0.5"
		C	Non-resilient	0.8"
		D	Plastic	1.0"
		E	Plastic	1.5"
		F	Plastic	1.5"
		G	Plastic	1.5"
		H	Non-resilient	0.5"
Facesheet Material ID		1	Fabric	0.5"
		2	Fabric	0.5"
		3	Fabric	0.5"
		4	Fabric	0.5"
		5	Rigid	0.5"

Cone calorimeter, ASTM E1354 [7], testing was conducted on the samples at an initial test heat flux of 50 kW/m². Average peak heat release rate and average heat release rate at 60, 180, and 300 seconds were recorded.

The rate of heat release is determined by measurement of oxygen consumption as determined by the oxygen concentration and the flow rate in the exhaust product stream, the heat evolved from the specimen per unit of time. The heat release rate ($\dot{Q}(t)$) is calculated by the following equation:

$$\dot{Q}(t) = \left(\frac{\Delta h_c}{r_o}\right) (1.10) C \sqrt{\frac{\Delta P}{T_e} \frac{(X_{O_2}^o - X_{O_2}(t))}{1.105 - 1.5X_{O_2}(t)}} \quad (2)$$

Where:

Δh_c = net heat of combustion, kJ/kg

r_o = stoichiometric oxygen/fuel mass ration (-)

C = calibration constant for oxygen consumption analysis, m^{1/2} - kg^{1/2} - K^{1/2}

ΔP = orifice meter pressure differential, PA

T_e = absolute temperature of gas at the orifice meter, K

X_{O_2} = oxygen analyzer reading, mole fraction O₂

The test specimen shall be 100 by 100 mm (4 inch by 4 inch) in area, up to 50-mm (2 inch) thick, and cut to be representative of the construction of the end-use product. For test samples of standard thickness greater than 50 mm (2 inches), the necessary specimen shall be obtained by cutting away the unexposed face to reduce the thickness to 50 mm (2 inches).

GVSC's intention is to measure the surface flammability, using ASTM E162 [9], of materials exposed to a prescribed level of radiant heat energy. Measuring surface flammability of materials employs a radiant heat source on a panel, 12 inch by 18-inch (305 mm by 457 mm). The orientation of the test specimen is such that ignition is forced near its upper edge and the flame front progresses downward. The test specimen shall be 6 inch by 18 inch (152 mm by 457 mm) by the sheet thickness, where this is less than 1 inch (25.4 mm). Materials supplied at a thickness greater than 1 inch (25.4 mm) shall be cut to 1 inch (25.4 mm) for testing.

A factor derived from the rate of progress of the flame front and another derived from the rate of heat liberated by the material under test are combined to provide a radiant panel index. The flame spread index takes into account the heat generated by the burning material after ignition. Heat generation is important to minimize in order to prevent the potential injury to mounted crew from inhaling hot air burning the lungs as well as from incurring severe skin and eye burn injuries.

ASTM E662 [8] employs an electrically heated radiant energy source mounted within an insulated ceramic tube and positioned so as to produce an irradiance level of 2.2 Btu/s· ft² (2.5 W/cm²) averaged over the central 1.5 inch (38.1 mm) diameter area of a vertically mounted test specimen facing the radiant heater. The nominal 3 inch by 3 inch (76.2 mm by 76.2 mm) test specimen is mounted within a holder which exposes an area

measuring $2 \frac{9}{16}$ inches by $2 \frac{9}{16}$ inches (65.1 mm by 65.1 mm). The holder is able to accommodate specimens up to 1 inch (25.4 mm) thick. This exposure provides the non-flaming condition of the test.

Specific optical density can be calculated at any given time as follows:

$$D_s = G \left[\log_{10} \left(\frac{100}{T} \right) + F \right] \quad (3)$$

Where:

$G = V/AL$

$V =$ volume of the closed chamber, ft^3 (or m^3)

$A =$ exposed area of the specimen, ft^2 (or m^2)

$L =$ length of the light path through the smoke, ft (or m)

$T =$ percent light transmittance as read from the light sending instrument

$F =$ depends on the movable filter used in the light path at time T is measured (a) $F = 0$ or (b) $F =$ the known optical density of the filter.

The specific optical density of smoke is calculated for both flaming and non-flaming modes for the material specimen.

3.4. Impact Speed

The target impact velocity is $6.6 \text{ m/s} \pm 0.27 \text{ m/s}$. The target velocity was derived from cadaveric UBB testing [4] conducted by the WIAMan program at Aberdeen Proving Ground (APG), Aberdeen, Maryland, using video tracking and analysis software. The target velocity represents the input velocity sustained on the cervical spine during UBB events. The use of $10 \text{ m/s} \pm 0.27 \text{ m/s}$ was to introduce an injurious impact velocity, whereas the input velocities of $3 \text{ m/s} \pm 0.27 \text{ m/s}$ and $5 \text{ m/s} \pm 0.27 \text{ m/s}$ represent non-injurious impact velocities during UBB events.

Due to the limitations of the component impact simulator (CIS) test fixture the non-injurious UBB event impact velocity of $3 \text{ m/s} \pm 0.27 \text{ m/s}$ was used.

The drop tower was released from approximately 1.47 m (57.8 inches) to achieve a pulse with the delta velocity of approximately 3 m/s. Additional tests were conducted to achieve a non-injurious impact velocity of approximately 5 m/s; however, the input threshold on the upper neck load accelerometer was exceeded. In order to minimize damage to laboratory equipment, only the impact velocity of 3 m/s was tested on the CIS test fixture.

The CIS test fixture was modeled in LS-DYNA to conduct testing at a higher impact velocity of approximately 3 m/s, 5 m/s, 6.6 m/s, and 10 m/s. The model of the CIS test fixture, Figure 3, is a simplified model of the test fixture.

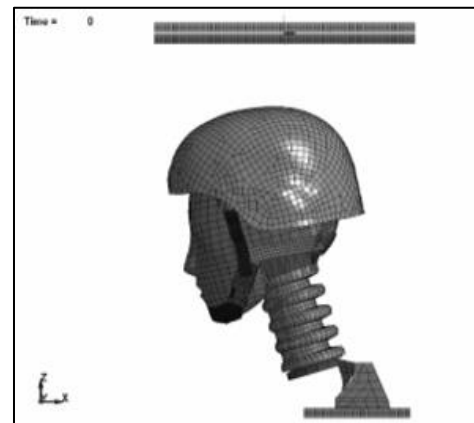


Figure 3: CIS LSDYNA Model for Test Evaluation, - 3.6 degree Flexion Neck Angle

The impact roof was modeled to be rigid and steel. The input plate, 8.8 kg, represents the carriage on the reaction tower. The lower neck load cell has a mass of 0.912 kg. The neck angle was measured between the front line of the neck section and the vertical z-axis.

Pearson's correlation defines the quantification of the degree to which two random variables are related assuming the relationship between the two variables is linear (Pagano *et al.* 2000 [13]). The Pearson's correlation coefficient gives an index of magnitude of the relationship between the

variables. The larger the absolute value of the correlation the stronger the relationship.

Pearson’s correlation was performed on the laboratory data and modeling and simulation data to measure the strength of the linear relationship between the two variables. Values near ± 1 are perfect correlation: as one variable increases, the other variable tends to also increase, if positive, or decrease, if negative.

3.5. Attachment Scheme

The roof liner attachment method was determined during Generic Hull (GH) testing conducted from February 10-12, 2015 in Fort Polk, Louisiana. Four different attachment schemes were tested on 12 inch by 12 inch energy attenuating (EA) materials located at three different locations in Generic Hull (GH) testing conducted, Figure 4. The attachment solutions tested were: click bond, fasteners, dual lock, and hook ‘n loop.

roof liner from 24 June 2019 through 16 July 2019. The 90 inch by 60 inch roof liner was mounted onto the fixture on the vibration exciter on the 6-DOF vibration table, to run all three major axis (longitudinal, transverse, and vertical) simultaneously, Figure 5. Low level vibration, at least 12 decibels (dB) below the vibration profile was applied. The vibration exciter, fixture, control system, and instrumentation system were fully functional.



Figure 5: Fixture used for vibration Testing, 90 inches by 60 inches

Seat 1		Seat 2	
Material 1: Baseline	Material 2 Attachment 1: Dual Lock	Material 1: Baseline	Material 2 Attachment 2: Hook 'n Loop
Material 3 Attachment 1: Dual Lock	Material 4 Attachment 1: Dual Lock	Material 3 Attachment 2: Hook 'n Loop	Material 4 Attachment 2: Hook 'n Loop
Seat 3		Seat 6	
Material 1: Baseline	Material 2 Attachment 3: Click Bond	Material 1: Baseline	Material 2 Attachment 4: Fastener
Material 3 Attachment 3: Click Bond	Material 4 Attachment 3: Click Bond	Material 3 Attachment 4: Fastener	Material 4 Attachment 4: Fastener

Figure 4: Generic Hull Headliner Attachment Scheme

3.6. Vibration

U.S. Army Redstone Test Center (RTC) Dynamic Test Division conducted vibration testing on the

4. RESULTS

4.1. Head Impact COTS Material

The primary focus of the testing was to evaluate the baseline head impact criteria of COTS materials. Each material tested was composed of a core material and facesheet material. The core material was identified with a core materials A through K. The facesheet material ID was identified 1 through 8. This material ID number represents a specific material configuration that was testing either on the flat fixture and/or on a vehicle for baseline testing.

The material samples with fabric exposed surface sheets generally performed better than the hard exposed surface sheet samples, facesheet materials 1 through 4, 6, and 7. Figure 6 shows the data from the flat fixture testing. The thicker core materials with fabric based surface sheets, core material IDs

D and E, performed below $HIC(d) \leq 1000$ requirement at $HIC(d)$ 636 to 855 for the 38 mm (1.5 inch) thick thermoplastic elastomer materials (TPE) engineered core material and $HIC(d)$ of 847 to 1131 with the 41 mm (1.6 inch) thick aluminum non-resilient core material, core material ID I. The foam covered in fabric in 25.4 mm (1 inch) thick samples covered in fabric, core material G, also showed results around the $HIC(d)$ threshold at $HIC(d)$ 1088. None of the thinner samples tested performed below the $HIC(d)$ requirement, core material IDs B, C, F, H and J. The lowest $HIC(d)$ value of the thinner samples was $HIC(d)$ of 1254 which is a resilient plastic core material covered in fabric, core material ID B. The thin material samples, core material IDs B, C, F, H, and J, with hard surface sheets, facesheet material IDs 5 and 8, showed significantly higher test results with the lowest $HIC(d)$ value of 1768.

core material ID I, resulted in an average $HIC(d)$ of 919.

4.2. Flame, Smoke, and Toxicity (FST)

The primary focus of the testing was to evaluate the flame, smoke, and toxicity criteria of COTS materials. Each material tested was composed of either a core material or facesheet material. The core material was identified with a core material ID A through H. The facesheet material ID was identified 1 through 5.

The net heat of combustion is directly related to the amount of oxygen required for combustion. The relationship is that approximately 13.1×10^3 kJ of heat are released per 1 kg of oxygen consumed. Specimens in the test are burned in ambient air conditions, while being subjected to a predetermined initial test heat flux, which can be set from 0 to 100 kW/m^2 . The test permits burning to occur either with or without spark ignition. Figure 7 illustrates the effect of heat release rate on the test specimens under an initial test heat flux of 50 kW/m^2 being representative of a military fire environment. The average heat release rate for all the facesheet material exceed the threshold requirement ranging from 430 kW/m^2 to 771 kW/m^2 . Seven of the eight core material exceeded the threshold requirement, 296 kW/m^2 to $1,019 \text{ kW/m}^2$. Core material H had an average peak release rate of 82 kW/m^2 , meeting the threshold criterion shown in a yellow line.

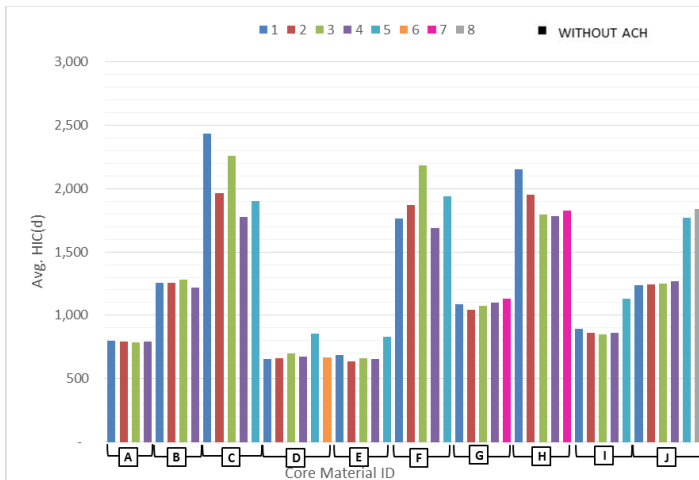


Figure 6: Material AoA HIC(d)

One of the TPE engineered materials, core material ID A, test results showed an average $HIC(d)$ of 792 at a thickness of 35.56 millimeters (1.4 inches). A non-resilient material, core material IDs I and J, (does not retain fit and form after impact) such as aluminum formed in a tubular shape, also uses air-space for enhanced energy attenuation. The 40mm (1.6 inches) thick non-resilient material,

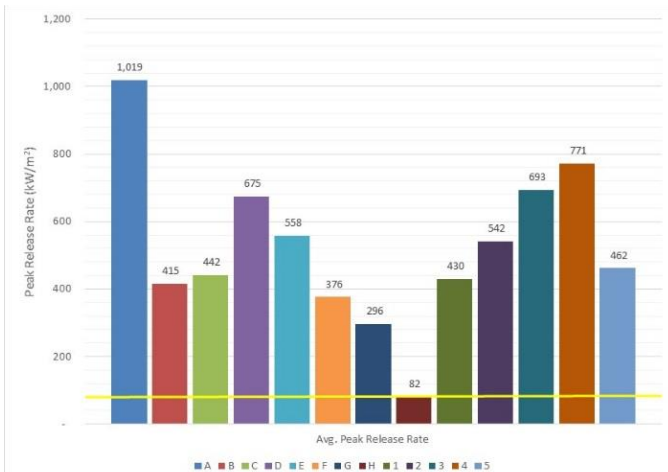


Figure 7: Average Heat Release Rate

The primary measurements taken through the cone calorimeter testing are oxygen concentrations and exhaust gas flow rates. Figure 8 shows the measurements taken at time intervals: 60 second, 180 seconds, and 300 seconds. At the time intervals of 60 and 180 seconds, only the core material ID H meets the threshold requirement. At 300 seconds, two core material IDs and four facesheet material IDs meet the thresholds requirement due to the flame being extinguished prior to the specified time point.

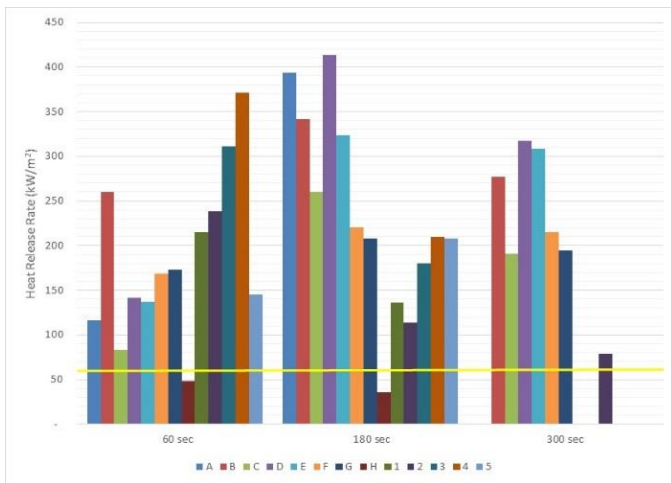


Figure 8: Effect of Heat Release Rate on Material

Flame spread index of a test specimen is the product of the flame spread factor, F, and the heat evolution factor, Q. The heat evolution factor is the

rate of heat liberated by the material, while the flame spread factor is the rate of progress of the flame front.

If flame spreads from the pilot burner position to the first 3 inch mark or from any 3 inch mark to the next in three seconds or less, is denoted with the term flashing. Figure 9 illustrates the flame spread index and whether flashing occurred during the test.

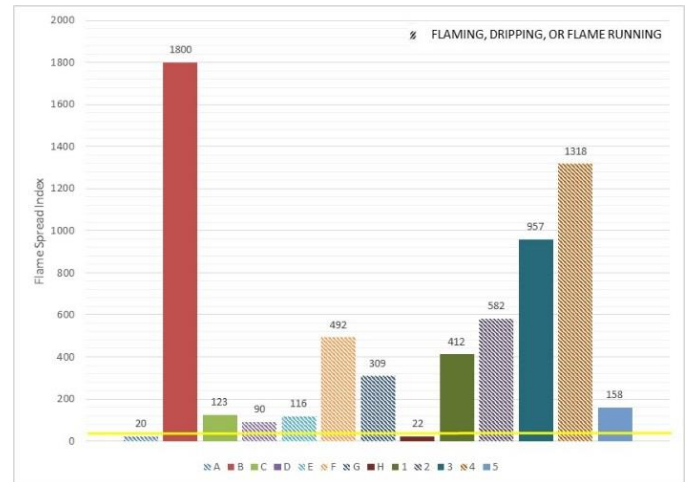


Figure 9: Effect of Flame Spread Index on Material

Seven of the thirteen materials tested experienced flaming, dripping, or flame running during the flame spread index tests. Core material ID A experienced flaming, dripping, or flame running and also met the threshold requirement with a flame spread index of 20. The remaining six material IDs D, E, F,G, 2, and 4 had a flame spread index ranging from 90 to 1,318.

The remaining six materials did not flame, drip, or flame run while being tested for flame spread index. Core material ID A met the threshold requirement with a flame spread index of 22. Material IDs B, C, 1, 3, and 5 had a flame spread index of 123 to 1,800.

Results are expressed in terms of specific optical density which is derived from a geometrical factor

and the measure optical density, a measurement characteristic of the concentration of smoke. Flaming optical density condition is derived from using a six-tube burner to apply a flames across the lower edge of the exposed test specimen. Figure 10 shows the results of the materials tested in the flaming condition.

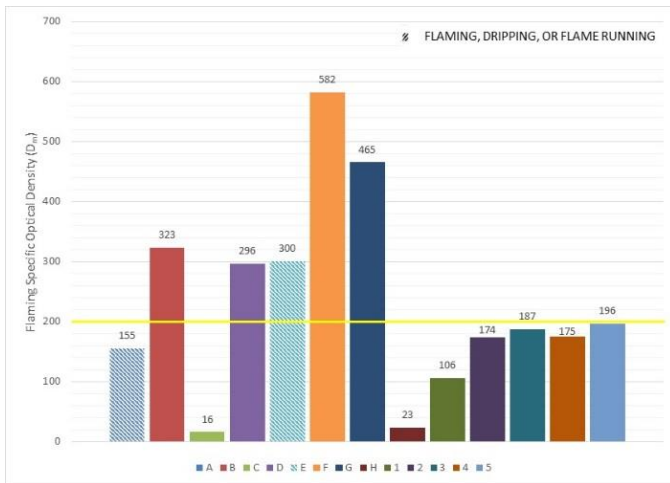


Figure 10: Flaming Specific Optical Density

All five of the facesheet materials tested met the threshold requirement of specific optical density less than 200 with results ranging from 106 to 196. None of the facesheet materials experienced flaming, dripping, or flame running while being tested. Core material IDs A and E experienced flaming, dripping, or flame running during testing. Core material ID A and C met the threshold requirements with a specific optical density of 155 and 16 respectively.

Non-flaming mode used a radiant heat source to produce the irradiance level of 2.2 Btu/s-ft² (2.5 W/cm²). Figure 11 illustrates the test specimens from the non-flaming condition. Core material ID F was the only material that did not meet the threshold requirement with a specific optical density of 320. All other materials met the threshold requirement with a specific optical density range of 1 to 185. None of the materials

tested flamed, dripped, or experienced flame running while in the non-flaming mode.

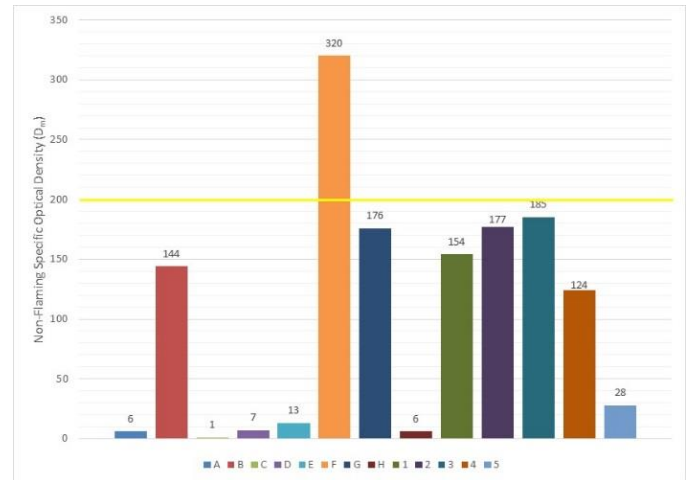


Figure 11: Non-Flaming Specific Optical Density

4.3. Impact Velocity

Forty eight different test configurations were used for modeling and simulation testing conducted by GVSC's Analytics Systems Engineering department. The primary goal of conducting modeling and simulation is to test configurations that are beyond the capability of the test equipment that more accurately represent conditions found in theater.

The compression force (F_z) is shown in Figure 12 for all tests conducted for modeling and simulation. For the test series with an input velocity of 3 m/s the average compressive forces exerted on the upper neck are 6,170 N at 12.7 mm clearance, 5,980 N for 25.4 mm clearance, 5,762 N for 50.8 mm clearance, and 5,400 N for 76.2 mm helmet to roof clearance. The average compressive force with an input velocity of 5m/s with helmet to roof clearances of 12.7 mm, 25.4 mm, 50.8 mm, and 76.2 mm are 12,139 N, 12,150 N, 12,164 N, and 12,041 N respectfully. Input velocity of 6.6 m/s, the average compressive forces exerted on the upper neck are 16,296 N at 12.7 mm clearance, 16,402 N for 25.4 mm clearance, 16,356 N for 50.8 mm clearance, and 16,263 N for 76.2 mm helmet to roof

clearance. The average compressive force with an input velocity of 10m/s with helmet to roof clearances of 12.7 mm, 25.4 mm, 50.8 mm, and 76.2 mm are 23,961 N, 24,096 N, 24,096 N, and 23,532 N respectfully.

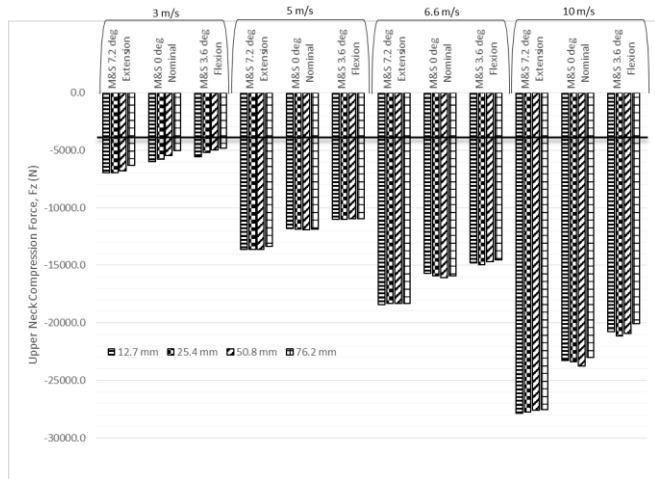


Figure 12: Modeling and Simulation Compression Force (F_z) for all data sets

The compressive forces by neck orientation are shown in Figure 13. For the test series at an input velocity of 3 m/s the average peak compression force was 6,764 N with a neck angle of 7.2 degrees, 5,576 N 0 degree neck angle, and 5,143 N -3.6 degree neck angle. The average peak compression force for the tests conducted at 5 m/s is 13,545 N the neck angle was 7.2 degrees, 11,849 N 0 degree neck angle, and 10,977 N -3.6 degree neck angle, flexion and extension. The 6.6 m/s input velocity test series had an average peak compression force of 18,332 N with a neck angle of 7.2 degrees, 15,914 N 0 degree neck angle, and 14,742 N -3.6 degree neck angle. The average peak compression force for 10 m/s is -27,681 N with a neck angle of 7.2 degrees, 23,362 N neck angle of 0 degree, 20,721 N neck angle -3.6 degrees.

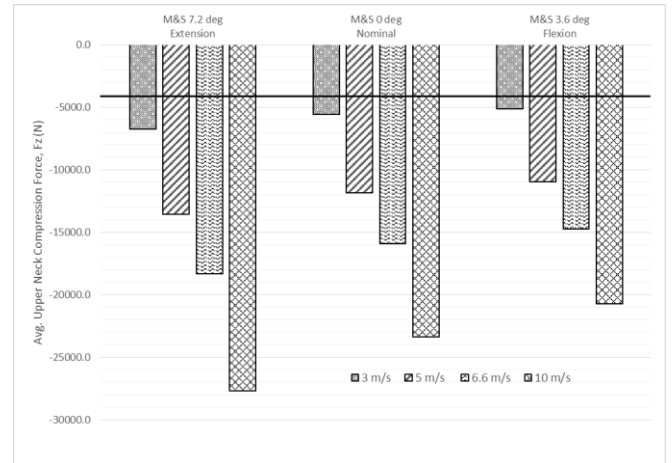


Figure 13: Modeling and Simulation compression force (F_z) for all data sets by neck angle

The average head injury criterion (HIC) for the modeling and simulation tests are shown in Figure 14. For the test series with an input velocity of 3 m/s the average HIC are 266 at 12.7 mm clearance, 240 for 25.4 mm clearance, 204 for 50.8 mm clearance, and 177 for 76.2 mm helmet to roof clearance. The average compressive force with an input velocity of 5 m/s with helmet to roof clearances of 12.7 mm, 25.4 mm, 50.8 mm, and 76.2 mm are 1,536, 1,339, 1,132, and 880 respectively. Input velocity of 6.6 m/s, the average compressive forces exerted on the upper neck are 2,903 at 12.7 mm clearance, 2,789 for 25.4 mm clearance, 2,722 for 50.8 mm clearance, and 2,322 for 76.2 mm helmet to roof clearance. The average compressive force with an input velocity of 10 m/s with helmet to roof clearances of 12.7 mm, 25.4 mm, 50.8 mm, and 76.2 mm are 8,261, 7,656, 7,760, and 7,448 respectively.

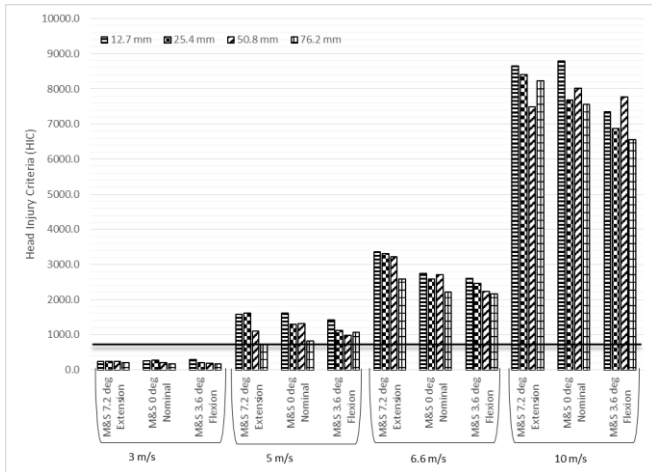


Figure 14: Modeling and Simulation HIC for all data sets

The HIC by neck orientation are shown in Figure 15. For the test series at an input velocity of 3 m/s the average HIC was 226 with a neck angle of 7.2 degrees, 225 0 degree neck angle, and 213 -3.6 degree neck angle. The average HIC for the tests conducted at 5 m/s is 1,259 the neck angle was 7.2 degrees, 1,259 0 degree neck angle, and 1,148 -3.6 degree neck angle. The 6.6 m/s input velocity test series had an average HIC of 3,117 with a neck angle of 7.2 degrees, 2,564 degree neck angle, and 2,371 -3.6 degree neck angle. The average HIC for 10 m/s are 8,193 with a neck angle of 7.2 degrees, 8,015 neck angle of 0 degree, 7,135 neck angle - 3.6 degrees.

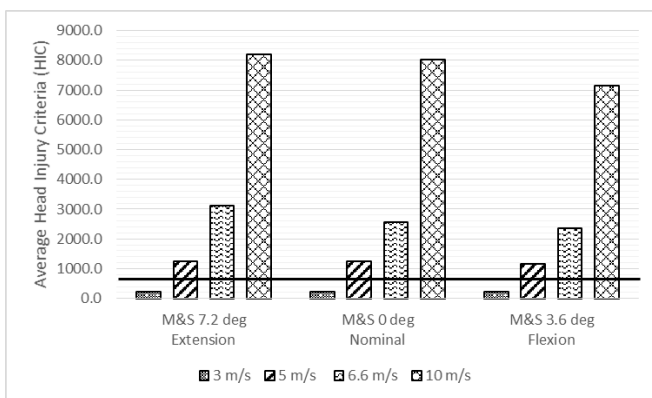


Figure 15: Modeling and Simulation HIC by neck angle

A strong degree of correlation for the Pearson’s coefficient value lies between ± 0.50 and ± 1.0 ,

moderate degree of correlation lies between ± 0.30 and ± 0.49 , and a low degree of correlation lies below ± 0.29 . The analysis showed a correlation coefficient of 0.845 between the laboratory data and the modeling and simulation for the upper neck (Fz) compression data.

The data analysis shows a Pearson’s correlation coefficient of 0.93 between the laboratory data and modeling and simulation for HIC at an impact velocity of 3 m/s.

4.4. Attachment Scheme

The three materials selected to be tested were three different masses, as shown in Figure 16. The fasteners and dual lock did not successfully hold all three materials in place during testing. Two attachment solutions, click bond and hook ‘n loop, passed the UBB and were able to keep the EA material in place under the forces exerted on them by the UBB.

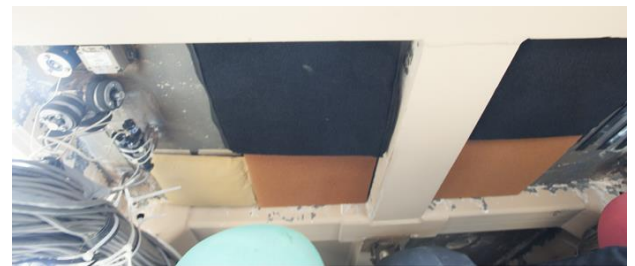


Figure 16: Generic Hull Seat Configuration

4.5. Vibration

RTC Dynamic Test Division personnel conducted visual inspections during the testing prior to and upon completion of the testing, Figure 17. No visual detachment of the roof liner was found.



Figure 17: Pre Test

5. Discussion

5.1. Head Impact COTS Material

Core material thickness appears to be the main characteristic affecting HIC(d) energy attenuating performance independent of the type of surface sheet material or attachment method as seen in Figure 18. The thicker core materials performed better than the thinner core materials. The average peak value of HIC(d) for the materials with a thickness of 12.7 mm (0.5 inches) is 1,953. The materials with a thickness of 25.4 mm (1 inch) has an average peak value of HIC(d) equal to 1,088. As the core material increases its thickness to 38.1 mm (1.5 inches) the average peak HIC(d) value continues to decrease to 693, supporting the observation that a thicker material reduces the head impact criterion. Looking at the materials with a thickness of 25.4 mm (1 inch) and less have an

average peak HIC(d) value of 1,612. Whereas materials with a thickness of greater than 25.4 mm (1 inch) has an average peak HIC(d) value of 772. The material thickness threshold for achieving the head injury criteria is greater than 25.4 mm (1 inch).

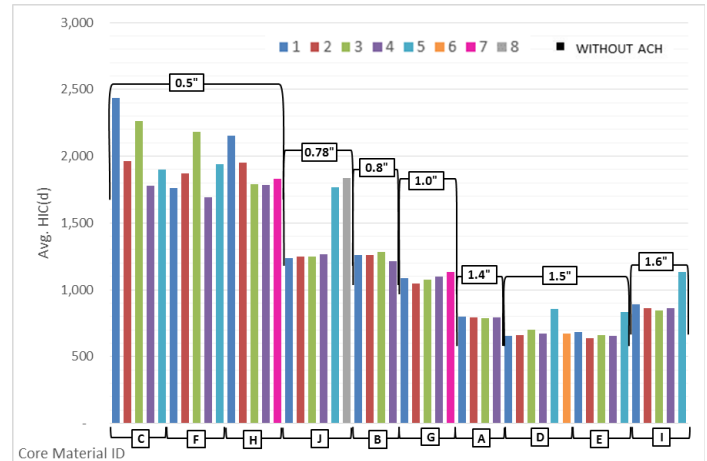


Figure 18: AoA Flat Fixture Material Thickness

Only some of the fabric based surface sheet samples with the low profile core material thickness, performed below the threshold $HIC(d) < 1000$ requirement and only one of the hard surface sheet samples with low profile core materials achieved the threshold requirement. These observations indicate the low profile core materials are more sensitive to the type of surface sheet material used, than the high profile, thicker core materials. AoA Test Material Matrix, Table 1, shows that facesheet material 1 through 4, 6, and 7 are fabric and facesheet material IDs 5 and 8 are rigid. Figure 19 shows core material ID J with a thickness 19.8 mm (0.78 inches) and how the fabric and rigid face sheets directly affect the core material's response to the injury criteria. The rigid face sheet increases the HIC(d) by an average of 553.

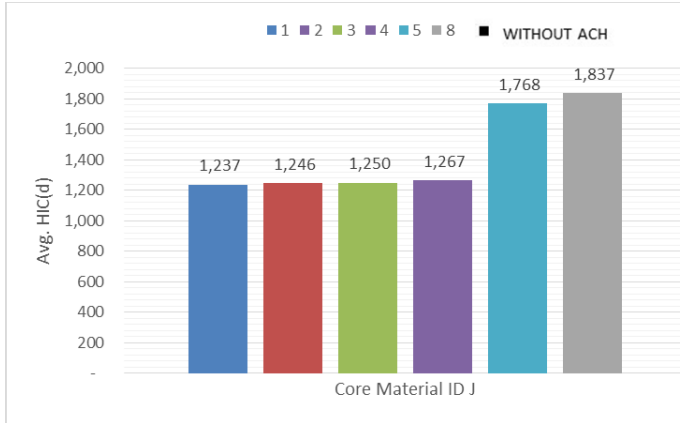


Figure 19: Core Material ID J, 19.8 mm (0.78 inch) thickness

5.2. Flame, Smoke, and Toxicity (FST)

Material thickness appears to not be a characteristic affecting the peak heat release rate of the test specimens. Figure 20 shows the test specimen broken out into the four material thickness tested: 0.5 inches, 0.8 inches, 1.0 inch, and 1.5 inches.

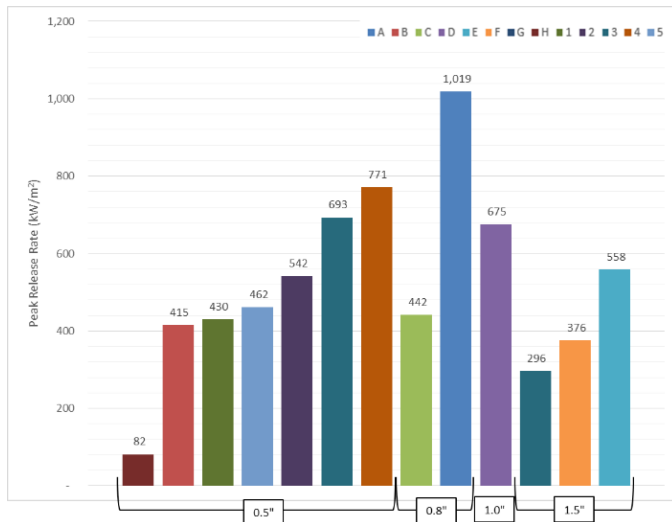


Figure 20: Cone Calorimeter Material Thickness

The average peak release rate of test specimens with a thickness of 0.5 inches is 485 kW/m², while test specimens of thickness ranging from 0.8 inches, 1.0 inch, and 1.5 inches have an average peak release rate of 730, 675, and 410 kW/m² respectively. This information states that materials

with a thickness of 0.5 and 1.5 inches have similar peak release rates, while materials experiencing a thickness between 0.5 and 1.5 inches have a higher peak heat release rate. This finding lead to the comparison of material properties to attempt to find a correlation in average peak release rate between materials tested.

Figure 21 looks at the material composition of the test specimens. The honeycomb Material H is the only test specimen that meets the requirement of an average peak release rate less than 85 kW/m². Foam, 415 kW/m², aluminum wire coated material, 442 kW/m², composite material, 462 kW/m², TPE sealed laminate, 476 kW/m², and polyurea, 609 kW/m², based materials all have similar average peak release rates. Material A, TPE, exceeded the threshold requirement by 1,098% with an average peak release rate of 1,019 kW/m².

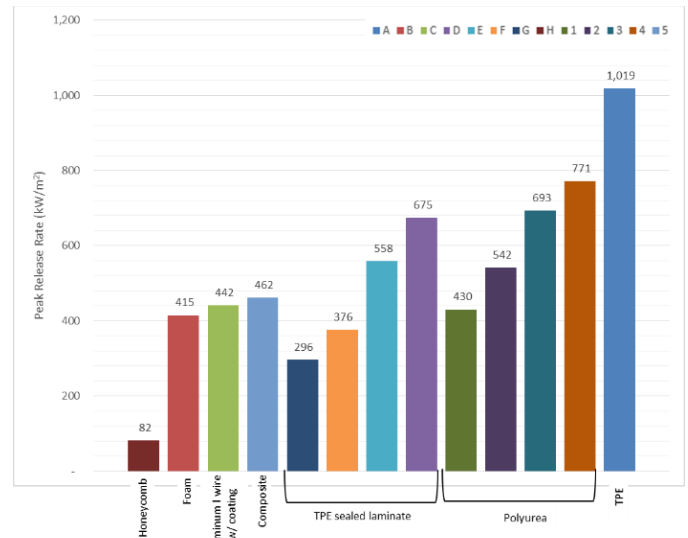


Figure 21: Cone Calorimeter Material Composition

The surface flammability testing shows the rate of progress of the flame front and the energy dissipated from the flame progression. Figure 22 shows the materials with a thickness of 0.5 inches have a greater flame spread index, 750. However the only material that passes the threshold

requirement without flaming, dripping, or flame running has a thickness of 0.5 inches.

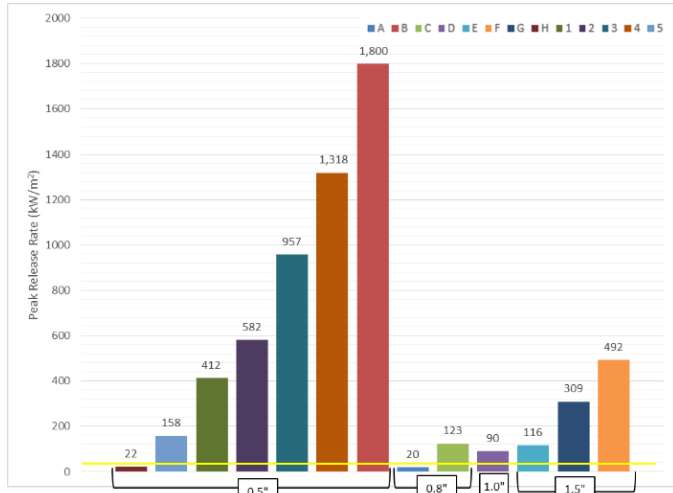


Figure 22: Flame Spread by Material Thickness

Comparing the test specimens by material composition showed that only TPE and honeycomb materials met the threshold criteria, Figure 23. Polyurea and foam materials performed the far exceeded the requirement with percent reduction in flame spread ranging from -1,274% to -5,900%. The laminate in the TPE reduced the percent of reduction by -739 percent, -707 percent from the TPE without laminate seal.

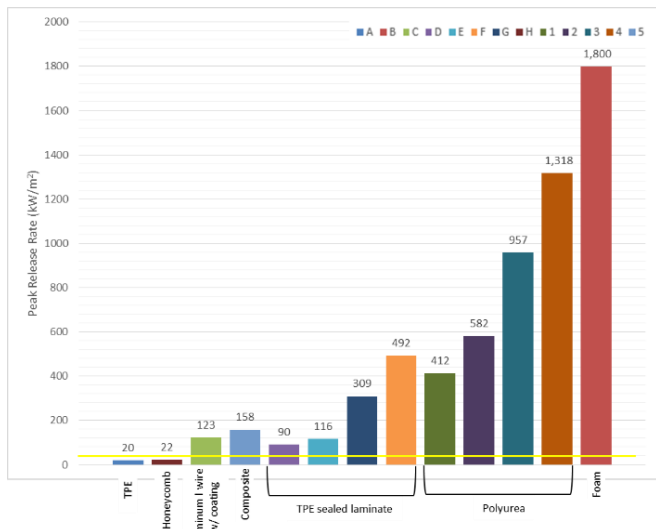


Figure 23: Flame Spread by Material Composition

Material A and H passed the flame spread index criteria. The difference between the two materials is that material A started to flame, drip, and flash 60 seconds into the test, Figure 24. Materials passing the required criterion while flaming, dripping, and flame running could potentially create a secondary injury. This phenomenon would render the material as not meeting the criterion.



Figure 24: Material A Flaming, Dripping, and Flame Running at 60 sec

Test specimens were tested for specific optical density using a flaming mode, Figure 25. Test specimens comprised of foam and TPE sealed with laminate failed to meet the threshold requirement. Composite, polyurea, TPE, honeycomb, and aluminum wire materials met the threshold requirement in the flaming mode. Two of the TPE and TPE sealed with laminate materials experienced flaming, dripping, and flash running.

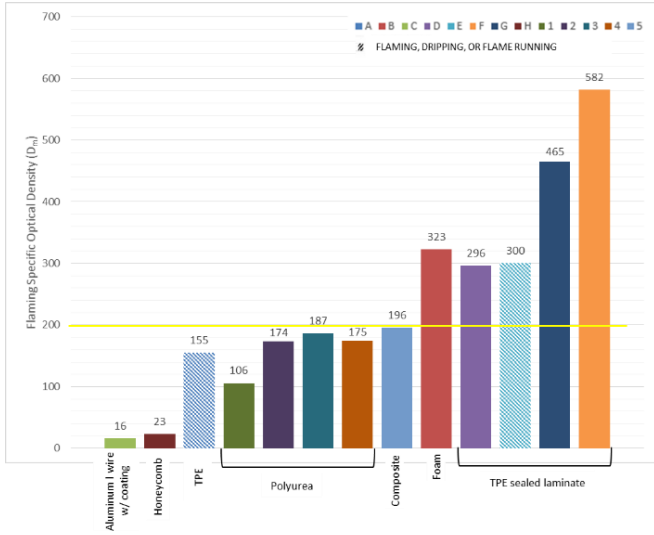


Figure 25: Flaming Mode by Material Composition

Test specimens tested in non-flaming mode for specific optical density all meet the threshold criterion with the exception of Material F. Material F is a TPE sealed laminate with a thickness of 1.5 inches. Figure 26 and 27 show the non-flaming test specimens broken down by material composition and thickness respectively.

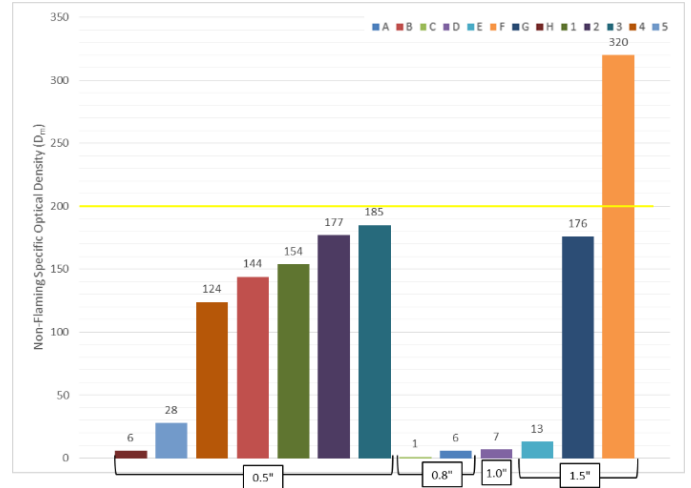


Figure 27: Non-Flaming Mode by Material Thickness

Materials E and G also have a thickness of 1.5 inches and meet the threshold requirement. Materials D, E, and G are also composed of TPE with laminate and meet the threshold requirement for specific optical density.

5.3. Impact Velocity

Data analysis was conducted on the upper neck compression force at an impact velocity of 6.6 m/s. The impact velocity of 6.6 m/s is input velocity found acting on cadaveric cervical spines during UBB events from video tracking of PMHS blast data. Figure 28 illustrates compressive force exerted on the upper neck with 12.7 mm to 72.6 mm of clearance between the helmet and roof. All compressive force values relating to helmet to roof clearance are at least three times greater than the threshold requirement. The difference between the highest and lowest compression force is 139 N.

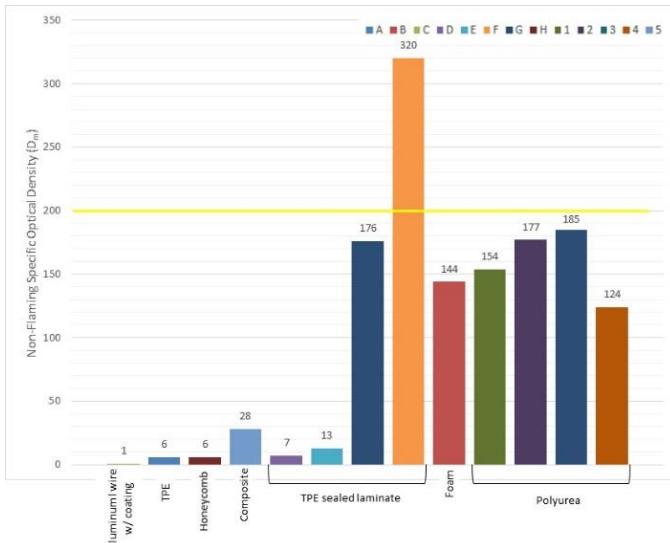


Figure 26: Non-Flaming Mode by Material Composition

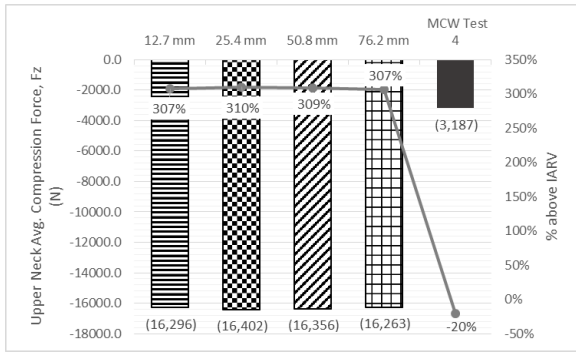


Figure 28: Upper Neck Force (F_z) by Helmet to Roof Clearance at 6.6 m/s

The compression force for 7.2 degree extension neck angle resulted in the highest compression force, 358% above the threshold requirement. Figure 29 shows how neck angle influences compression force at 6.6 m/s. The neck angle of -3.6 degrees flexion resulted in compressive force 269% above the threshold requirement, while the nominal 0 degree neck angle was 298% above the threshold requirement.

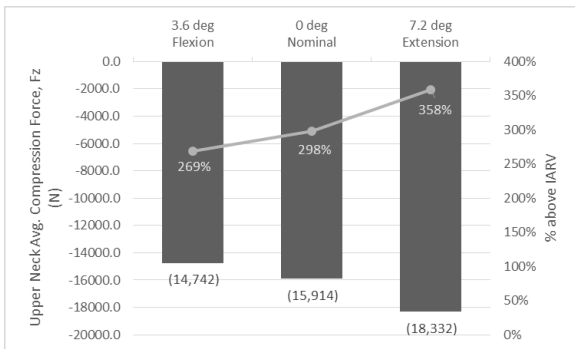


Figure 29: Upper Neck Force (F_z) by Neck Angle at 6.6 m/s

The HIC values at the injurious impact velocity on 6.6 m/s exceed the injury criteria by a factor of 3, Figure 30. The helmet to roof clearance parameter isn't as predominant of an influence in the HIC value as the non-injurious impact velocities. The clearances 12.7 to 50.8 mm have similar HIC values exceeding the injury criteria, while the greatest helmet to roof clearance, 76.2mm, is roughly 69% less severe; however, it still exceeds the injury criteria by 232%.

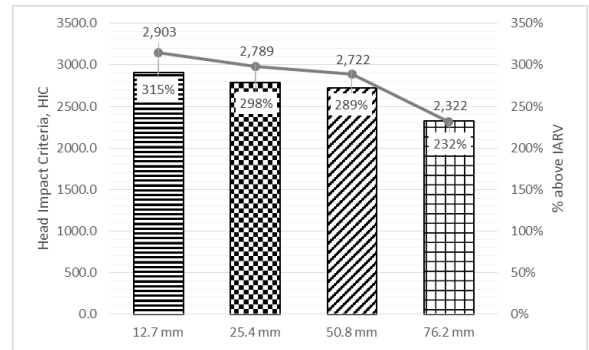


Figure 30: HIC by Helmet to Roof Clearance at 6.6 m/s

Neck orientation for injurious impact velocities is the parameter influencing the severity of injury. Extension neck orientation is the main parameter influencing HIC, Figure 31, with HIC of 345% greater than the injury criteria.

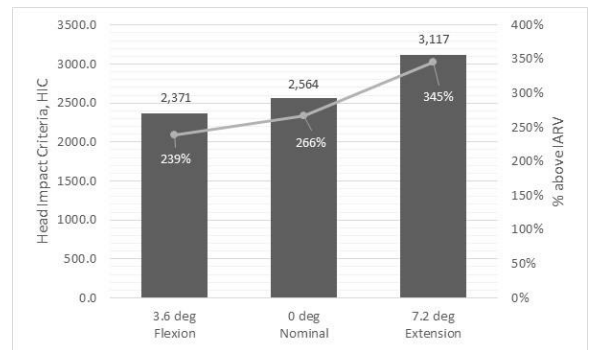


Figure 31: HIC by Neck Angle at 6.6 m/s

5.4. Attachment Scheme

Two attachment solutions, click bond and hook 'n loop, passed the UBB and were able to keep the EA material in place under the forces exerted on them by the UBB. Hook 'n loop was selected to be used for the attachment solution due to the ease of installation and replacement after conferring with the Program Management (PM) office regarding their requirements for maintenance.

5.5. Vibration

No anomalies were noted during visual inspections prior to or upon completion of testing,

as shown in Figure 32. The roof liner successfully stayed attached throughout the vibration testing.



Figure 32: Post Test

6. CONCLUSION

The flat fixture and vehicle baseline testing and evaluation performed on COTS materials provided GVSC with an objective assessment of materials performance with respect to the head injury criteria. The vehicle baseline testing showed certain materials consistently reduced HIC while on a flat vehicle surface. Further studies need to be conducted to identify material ability to contour to corners.

Through the use of the Design Review Based on Failure Modes tool, the need for improved fire resistant materials when large overhead (i.e. roof) protective materials are incorporated into the

vehicle design is identified as an important design feature. The direction towards the use of fire resistant materials, although through the development efforts associated with this project modified and novel materials were developed which meet the needs of the Army.

The cone calorimeter test performed on the COTS materials allowed GVSC's GVSP to assess the heat release rate of each material. Correlations could not be drawn between the different materials tested in the cone calorimeter environment. In this test series heat release rate was examined, however ASTM E1354 has the ability to provide quantitative data that lend to further calculations, time to ignition, mass loss rate, visible smoke, effective heat combustion, and caloric content. This test measures parameters from the other tests resulting in GSS using ASTM E1354 as the first flame, smoke, and toxicity test conducted on COTS materials.

The heat flux used in surface flammability testing is selected, which is a less scientific approach. A clear pattern on how flame spreads across the material was not evident. ASTM E162 is tested in a vertical test sample position. The COTS materials tested will be used in the horizontal position. The surface flammability test showed material ID A meeting the threshold requirement yet was flaming, dripping, and flame running. The flaming, dripping, and flame running could cause a secondary thermal injury to the warfighter. The intent of introducing COTS material into the vehicle is to reduce injury not create a secondary injury. This leads to the conclusion that meeting the threshold requirement of less than 30 is not evidence enough to approve the COTS materials as passing the test.

Minimizing smoke density is vital in the ingress and egress of the warfighter in the vehicle. The flaming and non-flaming mode showed that COTS materials with TPE have a greater tendency to produce smoke. ASTM E162 testing showed that

TPE materials also drip, flame, and flame run. These tests show that TPE is not a viable consideration for introduction into the military vehicle's interior.

The increase of impact velocity is showing that the neck orientation is playing a role in the compressive loading. Extension compressive loading has a 43% greater likelihood of injury versus flexion compression loading. The compression force neck angle data for an impact velocity of 6.6 m/s shows the continuing trend that 7.2 degree extension is a more severe neck angle for compression injury, followed by -3.6 degree flexion, and lastly 0 degree nominal. As impact velocity increases into an injurious velocity, helmet to roof clearance does not play a role in the likelihood of injury to the neck.

The neck angle upon impact played a significant role in the severity of injury sustained, most notably in the injurious impact velocities. Extension neck orientation is consistent with the compression loading and HIC seen at 6.6 m/s, 5 m/s, and 3 m/s.

The attachment scheme testing conducted on GH showed that there are two options for roof liner attachments. Hook 'n loop was selected to be used for the attachment solution due to the ease of installation and replacement after conferring with Program Management (PM) office regarding their requirements for maintenance.

Vibration testing was completed to obtain and provide test data for a research effort to examine how the adhesive Velcro on the GVSP Headliner withstands vibration.

GVSC used the knowledge gained through this effort to create a general performance specification for interior head impact protection for use in U.S. Army ground system vehicles. This performance specification is based upon the subject knowledge to date. GVSC acknowledges the performance

specification requires further development of durability and fire resistance requirements. As such, GVSC continues to research and develop these requirements and materials which provide sufficient energy attenuating characteristics while also being resistant to fire, durable and capable of performing in U.S. Army ground system vehicle environments.

Mandating military performance specifications for EA roof liners can substantially reduce the likelihood of injury to the warfighter during vertical accelerative loading events. Working in conjunction with a vehicle program, vehicle specific performance standards, requirements, and protection location(s) can be identified. It is important for a roof liner material to meet MIL-PRF-32518A. Meeting the requirements outlined in the specification and detailed in this paper will result in a technology that will meet test readiness level (TRL) 4 through 6.

The key component when releasing a military performance specification is that there is a technology readily available that currently meets all the requirements of the specification. The intent and accomplishment of the SBIR was to in fact create a roof liner technology that would be representative of the military vehicle environment.

7. REFERENCES

- [1] *Laboratory Test Procedure for FMVSS 201U Occupant Protection in Interior Impact Upper Interior Head Impact Protection*. U.S. Department of Transportation, Office of Vehicle Safety Compliance, Washington D.C. 20590.
- [2] Klima *et al.* "Interior Head Impact Protective Components And Materials For Use In US Army Vehicles" Ground Vehicle Systems Engineering & Technology Symposium (GVSETS), Novi, MI August 2015.
- [3] Klima *et al.* "Flame, Smoke, and Toxicity Energy Attenuating Materials for Use in Military Vehicles" Society of Automotive

- Engineers, World Congress, Detroit, MI, April 2018.
- [4] Klima *et al.* “Neck Injury Response in High Accelerations and its Algorithmical Formalization to Mitigate Neck Injuries.” Stapp Car Crash Journal, vol. 61, November 2017.
- [5] (10-1-12 Edition). 571.302 Standard No 302; Flammability of Interior Materials. Safety Assurance, Office of Vehicle Safety Compliance. United States of America: Department of Transportation.
- [6] Fire and Toxicity Test Methods and Qualification Procedure for Composite Material Systems Used in Hull, Machinery, and Structural Applications Inside Naval Submarines. U.S. Department of Defense.
- [7] Standard Test Method for Heat and Visible Smoke Release Rates for Materials and Products Using an Oxygen Consumption Calorimeter. American Society for Testing and Materials. ASTM International.
- [8] Standard Test Method for Specific Optical Density of Smoke Generated by Solid Materials. American Society for Testing and Materials. American Society for Testing and Materials International.
- [9] (2012). Standard Test Method for Surface Flammability of Materials Using a Radiant Heat Energy Source. American Society of Mechanical Engineers. ASTM International.
- [10] (2008). Test Method Standard Environmental Engineering Considerations and Laboratory Tests. Department of Defense.
- [11] Fire and Toxicity Test Methods and Qualification Procedure for Composite Material Systems Used in Hull, Machinery, and Structural Applications Inside Naval Submarines. U.S. Department of Defense.
- [12] Prasad P, Mertz HJ. The position of the United States delegates to the ISO Working Group 6 on the use of HIC in the automotive environment. SAE 851246, 1985.
- [13] Pagano, M., Gauvreau, K. (2000). Principles of Biostatistics. 2nd edition. Duxbury Press; Belmont, CA.